GEISER

Geothermal Engineering Integrating Mitigation of Induced Seismicity in Reservoirs

www.geiser-fp7.eu

Grant Agreement no. *241321-2*

Geothermal Engineering Integrating Mitigation of Induced Seismicity in Reservoirs

Project Acronym: GEISER

D3.1 – Evaluation of systematic relations between the seismic responseto fluid injection and depth, injection pressure, crustal stress state, and local structural geology

Due date of deliverable: 31.03.2012
Actual submission date: 16.04.2012

Start date of project: 1.1.2010 Duration: 42

Participant short name: AMRA, BRGM, ETHZ, EOST, GFZ, INGV, ISOR, NORSAR

NAMES INVOLVED: A. Zang, V. Oye, Ph. Jousset, M. Bohnhoff, G. Kwiatek, J. Albaric, N. Deichmann, B. Goertz-Allmann, M. Calo, C. Dorbath, K. Agustsson, O. Flovenz, N. Maercklin

Revision: 1

DisseminationLevel		
PU	Public	x
PP	Restricted to other programme participants (including the Commission Services)	
RE	Restricted to a group specified by the consortium (including the Commission Services)	
CO	Confidential, only for members of the consortium (including the Commission Services)	

Table of Contents

1. EXECUTIVE SUMMARY

Evaluation of systematic relations between the seismic response to fluid injection and **depth, injection pressure, crustal stress state, and local structural geology**

The analysis of microseismic data from various EGS stimulations (Table 1) shows that a clear relationship exists between fluid injection and seismic response. A widely observed feature is that seismicity occurs first close to the injection well and then gradually propagates further away from the injection well. Detailed knowledge on the spatio-temporal distribution of the seismicity is strongly dependent on the properties of the physically installed seismic network, on the uncertainty in the assumed velocity model and on the applied methods for event location. For example, Kwiatek et al. (section3) re-analysed the Berlin, El Salvador dataset using the double-difference location algorithm and, although using the same data, they candraw new conclusions as compared to previous studies. One of their observations is that the Brune stress drops of events close to the injection point are smaller than the Brune stress drops of events that are further away from the injection point. A similar trend was observed by Goertz-Allmann et al. (2011, section 10) in the Basel, Switzerland, dataset. This data is further investigated by Bachmann et al. (section 11) and Goertz-Allmann and Wiemer (section 12). The seismic network has a strong influence on the quality of the event locations and obviously, seismic networks that comprise deep downhole sensors can detect and locate dramatically more events as compared to networks that solely consist of surface stations. The seismic network in Basel has six deep borehole stations with one three-component sensor deployed in each borehole, in addition to an extensive surface seismic network.Kraft and Deichmann (section 13)investigate how to improve the catalogue of about 3500 events using cross-correlation methods, solely using high-quality downhole data. They also compare estimated focal mechanisms from the downhole network with focal mechanisms estimated by the surface network.In yet another paper on Basel, by Zhao et al. (section 14),the authors studythe 19 largest events (LME) during and after the injection sequence and determine moment tensors from full waveforms. The analysis results in similar double-couple components as found by Deichmann and Ernst (2009), and in addition it reveals significant isotropic components during the early injection phase. Most of the events in the later stage are dominated by the double-couple components. The locations of the events with high isotropic components also coincide with previously found regions of high b-values and low Brune stress drops (Goertz-Allmann et al., 2011). It is therefore likely that a correlation between b-values, stress drops and isotropic components exists. Such relationship may help to explain discriminating between induced events (re-opening of existing fractures and creation of new flow paths) and triggered events (small stress perturbations on critically stressed faults result in failure).

Today's EGS reservoirs are mainly developed between 2 and 5 km depth (Table 1) and we do not observe a relation between the seismic activity and the depth of the reservoir, neither in the amount of recorded seismicity nor in the maximum measured magnitude. However, the depth of the reservoir needs to be taken into account when it is linked to the injection pressure and to the crustal stress state. In cases where several stimulation phases were conducted at the same well, seismicity seems to be reduced or is even absent until the stress level of previous stimulations is exceeded. This so-called Kaiser-effect has been pointed out by Baisch et al. (2010) for the Cooper Basin and is also observed by Kwiatek et al. (section 3) in the Berlin, El Salvador dataset. Calo et al. (section 8) observe that a previous stimulation may change the stress field for subsequent stimulations. They show that at

theSoultz-sous-Forêts site, France, the stress fieldaround the injection well might not be fully restored, which affects the seismicity patterns of secondary injection intervals.

In the beginning of most EGS projects, the information on local structural geology and the knowledgeof seismic velocities and densities is often poor. Especially the shear-wave velocities are often extrapolated from simple P-wave velocity models, resulting in high uncertainties in the event locations.Albaric et al. (section 4) discuss the importance to obtain a good understanding of the local structural geology already during the first stimulation phase. In their paper about a first hydraulic stimulation at the ParalanaEGS in Australia, the authors take advantage of several seismic 2D lines and some information from borehole logs. With this information, they construct a 3D velocity model for P- and S-wave velocities, which is then used to locate the microseismic events. They further conduct double-difference relocation fora subset of events. Finally they analyse focal mechanisms of selected events and find that the resulting double-couple components are in agreement with the regional compressive stress field.Jousset et al. (section 5) apply ambient seismic noise analysis to retrieve information about the structural model of the reservoir. Their study area is the Bouillante geothermal field, Guadeloupe, French Antilles, where generally little seismicity is associated to the geothermal exploitation. After implementation of the results from the ambient seismic noise tomography, the authors locate the few recorded microseismic events and discuss the source parameters in light of the reservoir model.

Due to active processes within geothermal reservoirs, changes of the physical properties over time are likely.Cooling of the rock, dissolution and precipitation processes after long term fluid circulation, seismic and aseismic deformation of the reservoir during stimulation and afterwards during circulation, are all processes that change rock properties. Detailed analysis of waveform data from The Geysers, California, USA, (Gritto and Jarpe, section 9 and section 15)reveal temporal changes of the Vp/Vs velocity ratio over time. The authors observe e.g. that an increase in Vp/Vs ratio along with a decrease of Vp and Vs velocities is indicative for fluid-filled fractured rock.Calo et al. (2011, section 6 and 7) conductedtime-lapse double-difference tomography at the Soultz-sous-Forêts site and found that aseismic deformation close to the injection site might have a significant contribution to the change in velocity values. In section 8, Calo et al. present event relocations from the GPK4 stimulations at Soultz-sous-Forêts, derived from double-difference methods. The temporal evolution of the relocated seismicity is grouped around the open–hole section of the injection well and the authors interpret this pattern with respect to the in-situ stress field.

The following sections are abstracts of articles, in most cases followed by an attachment with the full article, or a draft manuscript to be submitted to a special volume of Geothermics.

Sites analysed in GEISER	LME*, year	Geology, rock type, stress	P_{max}, MPa	Reservoir depth (km), fracture mechanism	Previous References
The Geysers , California USA	4.6, 1982	Metagraywacke	7	3 km, cooling-induced shear slippage, since 1975	Oppenheimer 1986, Rutqvist et al. 2010
Berlin, El Salvador	4.4, 2003	young volcanic weak rock	13	2 km, opening and closing of flowing fractures, since 1991	Bommer et al. 2006
Cooper Basin, Australia	3.7, 2003	granite with 3.6 km sediment cover, TF	68	4.1 to 4.4 km, slip on pre-existing sub-horizontal fractures, since 2003	Asanuma et al. 2005, Baisch et al. 2006
Alkmaar, NL	3.5, 2001	sandstones, 2.6 to 3.1 km depth	18	2 km, reactivation Roer Valley Rift faults, gas production since 1963	van Eck et al. 2006, Dost + Haak (2007)
Basel , Switzerland	3.4, 2006	granite, Sh= 0.7SV, SH – N144°E±14°	30	4.4 to 4.8 km, pre-existing,en-echelon-type shear zone, since 2006	Häring et al. 2008, Evans et al. 2011
Soultz-sous-Forets, France	2.9, 2003	granite, NF + SS SH – N170°E	16	4.5 to 5.0 km (GPK3), single large tectonic fracture zone, since 1987	Cuenot et al. 2008, Dorbath et al. 2009
Landau, Germany (non-GEISER)	2.7, 2009	crystalline/sedi-mentary rock Sh<SV, SH – NS	5	2.8 km, dilatants shear fractures, since 2005	Bönneman et al. 2010 (non-paper)
Paralana, Australia	2.5#, 2011	Sedimentary basin, with basement below 4km, TF	62	4 km, reverse fault events	Hasting et al., 2011, Albaric et al. (this issue)
Rosmanowes, Cornwall, UK	2.0, 1987	Carnmenellis granite batholite	16	2 km, system of natural fractures, since 1977	Pine + Batchelor 1984, Turbitt et al. 1987
KTB, Germany	1.2, 1994	gneiss, metagabbro SS (1-8km), SH – N160°E	53	9.1 km, scientific wells, dilatant shear cracks, since 1987	Zoback + Harjes 1997, Baisch + Harjes 2003
Groß-Schönebeck, Germany	-1.0#, 2007	Rotliegend sand-stone, volcanic rock NF, SH – N18°E	60	4.1 km, only a total of 80 seismic events detected, doublet in 2007	Huenges et al. 2006, Kwiatek et al. 2010

Seismic: *= local magnitude LME, #= moment magnitude LME
Hydraulic: P_{max}= maximum well head pressure
Stress: SH= maximum-, Sh= minimum horizontal-, SV= vertical in-situ stress, SH-Orientation (N°E)
Faulting type: NF= normal-, TF= thrust, SS= strike-slip faulting

Table 1:*Analysed geothermal sites within the GEISER WP3. Large magnitude events (LME) in deep crustal injection experiments are listed in decreasing order of local magnitude.*

2. Analysis of induced seismicity in geothermal reservoirs - an overview.

Zang A, Oye V, Deichmann, N, Goertz-Allmann B, Jousset Ph, Gritto R
to be submitted to Geothermics

Abstract: In this overview we present first results of analysing induced seismicity in geothermal reservoirs of various tectonic settings.Within the framework of the European GEISER project we stress two deliverables. (1) We evaluate systematic relations between the seismic response to fluid injection and depth, and three types of reservoir key parameters: type I in-situ state of stress and rock properties, type II local geological structures like faults, and type III hydraulic energy described by fluid volume injected and pore pressure. (2) We evaluate source characteristics of so-called large magnitude events and their occurrence in space and time. The estimated seismic cloud,as observed in geothermal reservoirs, is often used for further interpretation. However, the exact location and shape of such seismic clouds strongly depends on the seismic network installed, velocity model used and location technique applied. Source mechanisms determined fromdownhole and surface seismic networksindicate mode I (tensile) fractures in the early stimulation phase of a reservoir and mode II (shear) fractures in later treatments. Locations of events with isotropic components (mode I fractures) coincide with high *b*-values and low Brune stress drops. We rate in-situ stress as the most critical parameter in reservoir development and life-time after the presence of heat. This is because previous stimulations change near-well stresses, and multiplystimulated wells (in crystalline rock only) follow a kind of field Kaiser effect, where little or no seismicity is produced until the previous maximum stress level is exceeded. For the safe use of geothermal energy we recommend (1) to map the three-dimensional shape of local faults and seismic velocities down to the reservoir depth beforehand, or in the first stimulation phase by latest, (2) to investigate aseismic deformation close to the injection well, (3) to image V_P/V_S ratios in order to avoid a large flow path connecting the two wells, and (4) to avoid triggering of critically stressed faults at the edges of the stimulated reservoir, which poses the largest seismic risk.

3. High-resolution analysis of seismicity induced at Berlín geothermal field, El Salvador.

G. Kwiatek, F. Bulut, M. Bohnhoff, G. Dresen, S. Oates
to be submitted to Geothermics

Abstract: We investigate induced microseismic activity monitored at Berlín Geothermal Field (BGF), El Salvador, during a hydraulic stimulation. The site was monitored for a time period of 17 months using 13 3-component seismic stations located in shallow boreholes. Three stimulations were performed in the well TR8A with a maximum injection rate and well head pressure of 140 l/s and 130 bar, respectively. For the entire time period of our analysis, the acquisition system recorded 581 events with moment magnitudes ranging between -0.5 and 3.7. The initial seismic catalog provided by the operator has been substantially improved: 1) We re-picked P- and S-wave onsets and relocated the seismic events using the double-difference relocation algorithm based on cross-correlation derived differential arrival time data. Forward modeling was performed using a local 1D velocity model instead of

homogeneous full-space. 2) We recalculated source parameters using the spectral fitting method and refined the results applying the spectral ratio method. We investigated the source parameters and spatial and temporal changes of the seismic activity based on the refined dataset and studied the correlation between seismic activity and production. The achieved hypocentral precision allowed resolving the spatiotemporal changes in seismic activity down to a scale of a few meters. Of the special interest is the largest event (MW3.7) and its nucleation process. This event occurred in the center of the BGF about two weeks after the termination of the second injection in TR8A and is interpreted to be related or even triggered by the shut-in of the wells. This characteristics is in accordance with the occurrence of induced “larger magnitude events” in a number of other geothermal sites.

4. Microseismic monitoring of the first hydraulic stimulation phase at the Paralana geothermal field, Australia.

Albaric J., Oye V., Langet N., Kuehn D., Lecomte I., Hasting M., Messeiller M. and Iranpour K.
to be submitted to Geothermics

Abstract: Paralana is a new Enhanced Geothermal System (EGS) located in South Australia. An injection well was drilled into a 4 km thick sedimentary basin covering radiogenic basement. The first fluid injection aiming at enhancing a reservoir was performed in July 2011 and induced more than 7000 microearthquakes, which were automatically processed. A 3D velocity model was built using seismic reflection data to improve the location of events, whichcluster at the sediment-basement boundary at 4 km depth. The growth of the reservoir is indicated by the migration of earthquakes toward NE. Relocation of events with waveform cross-correlation data allowed a clear identification of two main fractures activated during two different phases of injection. The largest earthquake (Mw 2.5) occurred near the end of the second stimulation phase at the base of the entire seismic cloud.

See ATTACHMENT 1

5. Ambient seismic noise analysis: methodology and examples from Bouillante geothermal field.

P. Jousset, A. Bitri, M. Delatre, V. Bouchot, J. Vasseur,C. Contes, J. Loiseau and B. Sanjuan
to be submitted to Geothermics

Abstract: The knowledge of structuraland fluid dynamics of geothermal areas is fundamental in orderto increase the efficiency of targeting the resource, improve fluid recovery and manage the resource optimally. Micro-seismicity ingeothermal systems is one of the important indicators which give insightsin both structural features and dynamical behaviour of geothermal systems, i.e., better assess conditions that prevail to trigger Large Magnitude earthquakes.In order to locate accurately the micro-seismicity, the knowledge of the velocity field is of prime importance. We apply ambient seismic noise analysis with cross-correlation techniques at different geothermal sites to get insightsin structural features of geothermal systems. We retrieve the Green’s function, characteristic of the seismic velocity field of rocks,

using surface-wave tomography from the cross-correlation of ambient seismic noise. In order to monitor the reservoir dynamical features, we infer seismic velocity changes using waveform interferometry of the ambient noise. We apply cross-correlation of the ambient seismic noise to recover the Green's functions for Bouillante, Guadeloupe (French Antilles) exploited geothermal field.The geothermal field of Bouillante (Guadeloupe, French Lesser West Indies) is the only high temperature site exploited overall the French territory. Since 2004, a seismological network has enabled classification and analysis of continuous seismic data. In about 8 years or recording, very little micro-seismicity has been detected generated in the geothermal field, whereas intense seismicity is linked to the subduction processes.Cross-correlation technique is also accurate enough to resynchronize data with missing GPS, which then allow us to pick seismicity with accuracy better than picking error.We locate and characterize the few local micro-seismic events in terms of spectral frequencies, wave forms, ratios of seismic velocities, magnitudes, etc. We interpret these results in the light of the structural model of the reservoir.

6. Large scale aseismic motion identified through 4D P wave tomography.

M. Calò, C. Dorbath, F. Cornet, N. Cuenot. Geophys. J. Int., 2011

Abstract: In 2000, a large water injection (over 23 000 m^3) has been conducted in granite through a 5-km-deep borehole at Soultz-sous–Forêts, in the Upper Rhine Graben (northeastern France). The microseismicity induced by this hydraulic stimulation was monitored with a network of 14 seismic stations deployed at ground surface. Some 7215 well-located events have been used to conduct a 4-D tomography of *P*-wave velocities. The method combines a double-difference tomography method with an averaging post-processing that corrects for parameter dependence effects. The total set of 7 215 events has been divided into 14 subsets that explore periods defined with respect to the injection scheme. Particular attention is given to changes in injected flow rates, periods of stationary injection conditions and post-injection periods. Fast changes in $V_P$velocities are identified in large rock mass volumes precisely when the injection flow rate varies while little velocity variation is detected during stationary injection periods. The $V_P$anomalies observed during stationary injection conditions are interpreted as being caused by effective stress variations linked to fluid diffusion, while the fast changes observed concomitantly to changes in flow rate are considered to be caused by non-seismic motions.

See ATTACHMENT 2

7. Different behavior of the seismic velocity field at Soultz-sous-Forêts revealed by 4D seismic tomography: the case study of GPK3 and GPK2 injection tests.

M. Calò, C. Dorbath, F. Cornet, N. Cuenot. Geophys. J. Int., ready for submission.

Abstract: We present new results of a time-dependent (4-D) seismic tomography obtained with P- waves arrival times for seismic events recorded during the 2003 GPK3 stimulation. During this stimulation more than 7000 microearthquakes were recorded by the surface network. Among them we have selected 4728 events detected by the seismic network which had duration magnitude ranging from –0.9 to 2.9 and were accurately located. As Charlety et

al. (2006) did, we performed the 4-D seismic tomography after dividing the main set into chronological subsets to describe temporal changes in the seismic velocity structure during the stimulation. This study differs from theirs in three main points. First, the continuous seismic records were carefully reprocessed allowing a doubling of the events selected for the tomography. Second, the subsetting has been performed by taking into account variations of injection parameters (i.e. injection rate, wellhead pressure and downhole pressure). Third, the method combines a double difference tomography method (tomoDD, Zhang & Thurber 2003) with an averaging process (weighted average model (WAM), Calo', 2009) that corrects for parameter dependence effects.A comparison of these results with those of the 4D tomography obtained for the GPK2 injection test (Calo' et al. 2011) gives insights on the different response of the reservoir for the two wells.We discuss finally how the precise relocation of seismic events together with the temporal variations of the 3-D P-velocity models resulted able to better describe some already known features of the stimulated reservoir and to individuate new large structures.In conclusion we speculate that the large open fractures, some of them crossing GPK3, affected the repartition of the effective stresses around the well during the stimulation test. The presence of these structures, representing the main paths of the injected water, avoided the accumulation of effective stresses in the rock mass volumes close to GPK3. This resulted in a lack of large low Vp anomalies during the stimulation. The injected water involved a larger region activating structures away from the stimulation region as observed by the relocated seismicity and by the Vp velocity models. However a similar evolution occurred in the GPK3 and GPK2 stimulations when injected flow-rate was varied. This suggests that a similar mechanism for accommodating the increasing of the effectives stresses close to the wells occurs when sudden variations of flow rate are built during stimulations.

8. Injection tests at the EGS reservoir of Soultz-sous-Forêts. Seismic response of the GPK4 stimulations.

Calò M, Dorbath C, Frogneux M.
to be submitted to Geothermics

Abstract: The European Enhanced Geothermal System (EGS) programme of Soultz-sous-Forêts is organized around three wells (GPK2, GPK3, and GPK4) drilled to a depth of about 5000 m. Hydraulic stimulations were performed in the wells in order to increase the injectivity of the reservoir and the connectivity among the wells. The stimulation of GPK4 was achieved in two stages, in September 2004 and in February 2005. A network of 12 surface stations was deployed for the monitoring of the seismic response of the geothermal reservoir during both injection tests. These stimulations produced even less induced events than those of the other wells, making the interpretation difficult up to now. In this work we present some new observations on the seismicity of the GPK4 stimulations after a complete review of the seismic catalogues collected in 2004 and 2005. Furthermore, the events were relocated using double difference data. The new images of the seismicity are presented as temporal sequences according to the main variations of the injection parameters. The seismic events occurred during the 2004 stimulation are grouped in a dense cloud and centred on the well open-hole section. In 2005, the temporal evolution of the seismicity depicts a particular pattern suggesting that the "natural" stress field in the reservoir was not completely restored when the second injection test was performed.

See ATTACHMENT 3

9. Temporal Variations of VP/VS Ratio at The Geysers Geothermal Field, USA

Roland Gritto, Steven P. Jarpe
to be submitted to Geothermics

Abstract: A comprehensive database of earthquakes and associated phase arrivals was generated from data acquired by a 34-station seismic network at The Geysers geothermal field, USA, from 2004 to 2011. This database is comprised of several 100,000s events and 1,000,000s of P- and S-wave travel time picks. A high-precision sub-set of the earthquake data was selected to analyse temporal changes in seismic velocities and Vp/Vs-ratio throughout the entire reservoir. Relatively low Vp/Vs values, found for 2004 and 2005, were followed by a 6.3 % increase from 2005 to 2006, after which the Vp/Vs-ratio remained at the elevated level through 2011. The increase in Vp/Vs-ratio coupled with a decrease in P- and S-wave velocities from 2004 to 2011 is indicative of fluid-filled fractured rock. Coincidentally, the inception of a pipeline project to resupply the reservoir with water coincided with the first Vp/Vs-ratio measurements in 2004. It was found that the temporal variations in Vp/Vs-ratio reveal a high correlation to the total volume of injected water throughout the entire reservoir. Between 2004 and 2007, the observed correlation exhibits a one-year lag of the Vp/Vs-ratio relative to the injected water volume, while the correlation is near perfect between 2007 and 2011. The observed lag between Vp/Vs-ratio and fluid injection could possibly be used to estimate bulk permeability and storage capacity of the reservoir. Comparing the observed increase in Vp/Vs-ratio with an earlier study that reported a 9% decrease in Vp/Vs-ratio between 1991 and 1994, it can be concluded that three years after the inception of the pipeline project the fluid saturation appears to have been successfully increased throughout the reservoir.

10. Stress drop variations of induced earthquakesat the Basel geothermal site

Goertz-Allmann, B.P., A. Goertz, and S.Wiemer

We determine stress drops from P-wave spectra ofabout 1000 earthquakes induced by

hydraulic stimulationin crystalline rock for a deep heat mining project in Basel,Switzerland. We observe an increase in stress drop byabout a factor of five with radial distance from 10 m to300 m, which suggests that stress drop correlates withpore pressure perturbations due to the

injection. We testthis hypothesis by calculating the injection-related porepressure perturbation

based on a simple linear porepressure diffusion model and find a good correlation ofthe expected pore pressure perturbation with the estimatedstress drops.

See ATTACHMENT 4

11. Influence of pore-pressure on the event-size distribution of induced earthquakes

C.E. Bachmann,S.Wiemer,B.P. Goertz-Allmannand J. Woessner

During an Enhanced Geothermal System (EGS) experiment, fluid is injected at high pressure into crystalline rock, to enhance its permeability and thus create a reservoir from which geothermal heat can be extracted. The fracturing of the basement caused by these high pore-pressures is associated with microseismicity. However, the relationship between the magnitudes of these induced seismic events and the applied fluid injection rates, and thus pore-pressure, is unknown. Here we show how pore-pressure can be linked to the seismic frequency-magnitude distribution, described by its slope, the *b*-value. We evaluate the dataset of an EGS in Basel, Switzerland and compare the observed event-size distribution with the outcome of a minimalistic model of pore-pressure evolution that relates event-sizes to the differential stress *_D*. We observe that the decrease of *b*-values with increasing distance of the injection point is likely caused by a decrease in pore-pressure. This leads to an increase of the probability of a large magnitude event with distance and time.

See ATTACHMENT 5

12. Geomechanicalmodeling of induced seismicity source parameters and implications for seismic hazard assessment

Bettina P. Goertz-Allmann and Stefan Wiemer

We simulate induced seismicity within a geothermal reservoir using pressure-driven stress changes and seismicity triggering based on Coulomb friction. The result is a forward modelled seismicity cloud with origin time, stress drop, and magnitude assigned to each individual event. Our model includes a realistic representation of repeating event clusters, and is able to explain in principle the observation of reduced stress drop and increased b-values near the injection point where pore-pressure perturbations are highest. The higher the pore-pressure perturbation, the less critical stress states still trigger an event, and hence the lower the differential stress is before triggering an event. Less critical stress states result in lower stress drops and higher b-values, if both are linked to differential stress. We are therefore able to establish a link between the seismological observables and the geomechanical properties of the source region and thus a reservoir. Understanding the geomechanical properties is essential for estimating the probability of exceeding a certain magnitude value in the induced seismicity and hence the associated seismic hazard of the operation. By calibrating our model to the observed seismicity data we can estimate the probability of exceeding a certain

magnitude event in space and time and study the effect of the injection depth and crustal strength on the induced seismicity.

13. High-precision relocation and focal mechanism of the injection induced seismicity at the Basel EGS

Toni Kraft and Nicholas Deichmann
to be submitted to Geothermics

Abstract: In early December 2006, a massive fluid injection was carried out at 5km depth below the city of Basel, Switzerland, for geothermal reservoir enhancement. During the six-day stimulation, approximately 13000 induced microearthquakes where detected by a borehole network. The largest of the induced earthquakes, which had a magnitude of M_L 3.4, was strongly felt in the Basel area and led to the termination of the project after only 6 days of operation. We analysed the approximately 3500 locatable events of this induced earthquake sequence, which is one of the most densely monitored deep fluid-injections in the world. The seismic monitoring system consisted of six borehole seismometers at depths between 300 and 2700 m near the injection well and of numerous surface stations in the Basel area. In this article, we report on the analysis of the sequence using exclusively data from the down-hole instruments. We show how a refinement of arrival-time picks by cross-correlation techniques and subsequent high-precision relocations lead to significant improvements of the hypocenter locations compared to routinely adopted manual procedures. We also analyse focal mechanisms determined from both first-motion polarities and amplitudes of signals recorded by the borehole sensors alone and compare the results to the focal mechanisms of the larger events recorded also by the surface networks.

14. Full Waveform Inversion of Moment Tensor Solutions of the Induced Seismicity by the Stimulation of Enhanced Geothermal Site in Basel

Peng Zhao, Volker Oye, Daniela Kühn, and Simone Cesca
to be submitted to Geothermics

Abstract: Our study presents the results of moment tensor (MT) inversion of 19 strongest seismic events, associated with the enhanced geothermal reservoir stimulation operation at Basel, Switzerland (from 2 December, 2006 to 6 May 2007). We use the software package 'Kiwi' and adopt a three-step procedure to retrieve point solution parameters based on the waveform fit. After the first two steps, we obtain focal solutions, including hypocenter location, strike, dip, and rake of these 19 events assuming a double-couple source model. The results match well with the focal mechanisms estimated using the projections of first-motion polarities at about 40 seismic sensors. In comparison, less than 10 sensors near the injection well are used in the present study. In the last step, MT solutions of each event are solved using its best DC solution from the previous step as the initial model input. The isotropic components of MT solutions of some early events are not negligible, which could be caused by the volume change due to fluid injections. We also tempt to correlate the tempo-spatial patterns of isotropic components to the co- and post-stimulation processes of the Basel site. In this paper, we also investigate the influence of velocity model and station selection for the source inversion.

See ATTACHMENT 6

15.Re-analysis of microseismic data at The Geysers, California, USA

To validate available arrival time picks from NCEDC and to obtain a consistent data base of arrival times, the P-wave picks have been re-picked on vertical-component traces with an AIC-based maximum likelihood picker similar to the one described in Oye and Roth (2003). To this end about 200,000 validated P-picks with high accuracy are available for The Geysers in the period August 2007 through February 2011. The same method has been applied for S-waves, resulting in about 20,000 picks for the same period, indicating that more initial S-wave picks are required. Cross-correlation methods for picking and pick refinement have been tested, and for additional S-wave picking also polarization analysis and array methods shall be applied (Diehl *et al.*, 2009). In this respect some software procedures have been developed. The picks are currently used to cut out relevant portions of the waveforms for further analyses, and to select and relocate events.

Based on the micro-earthquake locations, their magnitudes, and their time occurrence, The Geysers have been divided into two seismic source zones, named Zone1 (NW) and Zone2 (SE), as shown in Figure 1. The separation has been verified by an analysis of the Gutenberg-Richter b-values using the Utsu test. Seismicity rate, minimum magnitudes of completeness (Mc), and b-values for the two zones were mainly calculated with the aim of seismic hazard analysis, but may also be useful for future studies on the characterization of the induced seismicity. The completeness magnitude Mc has been calculated using a maximum-likelihood technique, and b-values are estimated with the Aki (1965) technique with uncertainties according to Shi and Bolt (1982). Results for 2007–2010 are summarized in Figure 2. For the analysed years 2007–2010, the induced seismicity shows some seasonal variation, especially for Zone1, and systematic changes in the b-values are also observed, ranging from about 0.8 to 1.8. The completeness magnitude Mc is typically 1.2 or even smaller, and an improvement of the monitoring network toward later times is reflected in the data.

Besides that, the maximum expected magnitude Mmax in each of the two zones has been estimated, based on an energy-rate analysis proposed by Makropoulos and Burton (1983) for natural, regional earthquakes. The obtained estimates are Mmax 4.5 for Zone1 and Mmax 4.2 for Zone2, respectively. These values are consistent with longer-term seismicity and also with published geological information on Quaternary faults in the area (e.g. USGS and California Geological Survey, 2006).

Regarding the source parameters of induced micro-earthquakes, a multistep inversion procedure has been developed to invert displacement spectra for seismic moment *Mo*, corner frequency *fc*, and attenuation *Q*. In particular, the procedure can be outlined as follows: (1) Get initial values for *Mo*, *fc*, and source-receiver $t^*=T/Q$ from non-linear inversion of displacement spectra; (2) determine t^* by fixing event *Mo* and *fc*; (3) determine S-wave site response function from the average attenuation-corrected spectra at each station; (4) correct original spectra for site responses; and (5) compute final values of *Mo* and *fc* by inversion of site- and attenuation-corrected displacement spectra. The procedure has been successfully applied to natural earthquake sequences with a similar magnitude range, and it is now adjusted for application to induced seismicity at The Geysers. Results on source parameters are not yet available. It is planned to compute moments, stress drops, apparent stress, etc., and

to study the correlation between these parameters, their spatial and temporal distribution, and their relation with reservoir properties.

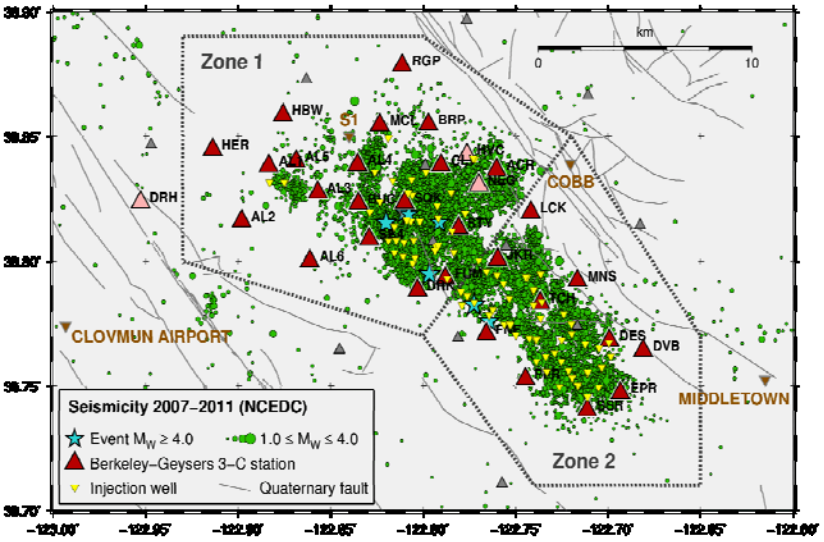

Figure 1: *Micro-earthquakes at The Geysers geothermal field between 2007 and 2011, seismic stations of the Berkeley-Geysers network, injection wells, and seismic source zones evaluated in seismic hazard analysis.*

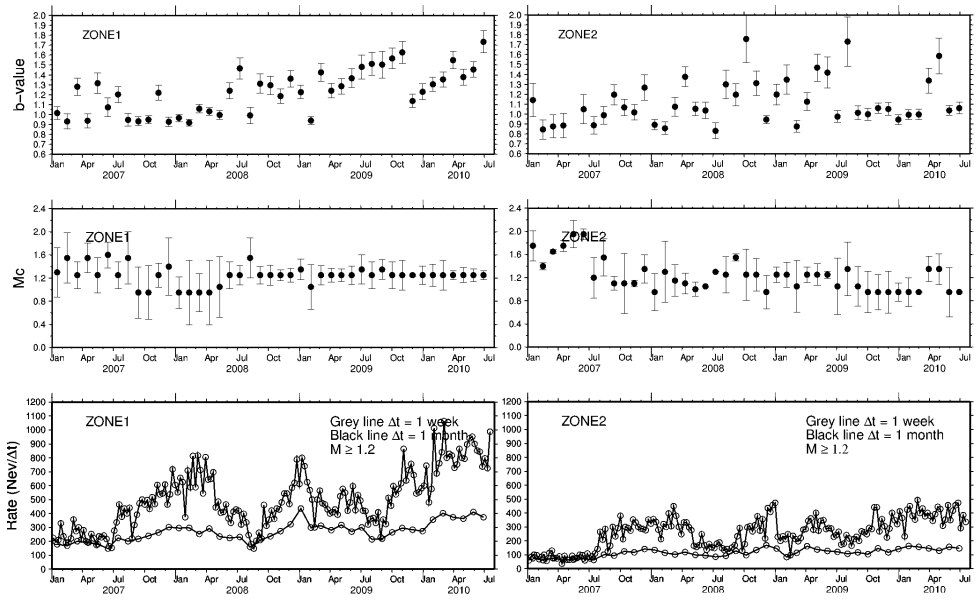

Figure 2: *Seismicity rate, magnitude of completeness (Mc), and b-values as a function of time for the two chosen seismicity zones at The Geysers geothermal field (Convertitoet al., 2011).*

16.Microseismic analysis of Icelandic geothermal field data

Seismicity data from three Icelandic geothermal fields, namely Krafla, Hengill and the Reykjanes peninsula, have been analysed. Data from Krafla that were obtained during the drilling of the IDDP well in 2009 have been analysed in some detail. The well was cased with a steel casing down to 1950 m and with a slotted liner around an aquifer at 1950-2080 depth at a top of a molten or partially molten magmatic intrusion. Low pressure stimulation with cold water during completion of the drilling and subsequent tests induced seismicity of magnitudes up to 1 in local magnitude. The epicentres initially followed the top of the magmatic layer horizontally away from the wellbore until it met an inclined fracture, most likely a pre-existing one. The epicentres then followed this fracture upwards showing the connection between the heat-mining zone at the top of the magmatic layer and the active fault systems. Furthermore, earthquakes in Krafla in 2010 have been located and are being analysed further.

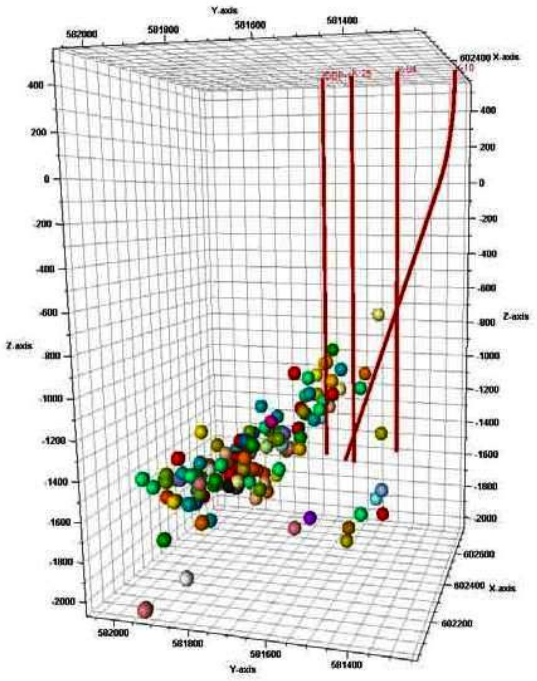

Figure 3*: Location of induced events around the IDDP well at Krafla during low pressure stimulation with cold water.*

The data from Hengill contain seismic and pressure recordings obtained during drilling of an injection well in February 2011 for the 303 MWeHellisheidi power plant in the Western part of the Hengill geothermal area. The injection well was drilled into a complex system of normal NE trending faults belonging to the axial rift zone of the Mid Atlantic Ridge in Iceland and N-S trending right lateral strike slip faults with character of the South Iceland transform zone. During the drilling, the well entered an open fracture at 1320m and total loss of circulation (40 L/s) was observed. A swarm of earthquakes was immediately initiated with magnitudes up to M_L 2.2. The earthquakes were clearly felt in the neighbourhood. These data are being analysed and will be used to shed light on the interaction between injection and pre-existing fractures. In September 2011 a full scale injection of 550 L/s started into the fissure swarm resulting in high level of induced seismicity. About 3000 earthquakes have been located in the area in 2011. The earthquakes came in intensive swarms with quiet intervals in between. The seismicity culminated on October 15th when several events of magnitude more

than 3.0 were measured, the largest one exceeding 3.8. This earthquake swarm occurred in conjunction with major disturbance of the injection rate. This is among the largest quakes that have been triggered by geothermal re-injection in the world. It caused serious inconvenience in a nearby village as people were not prepared.

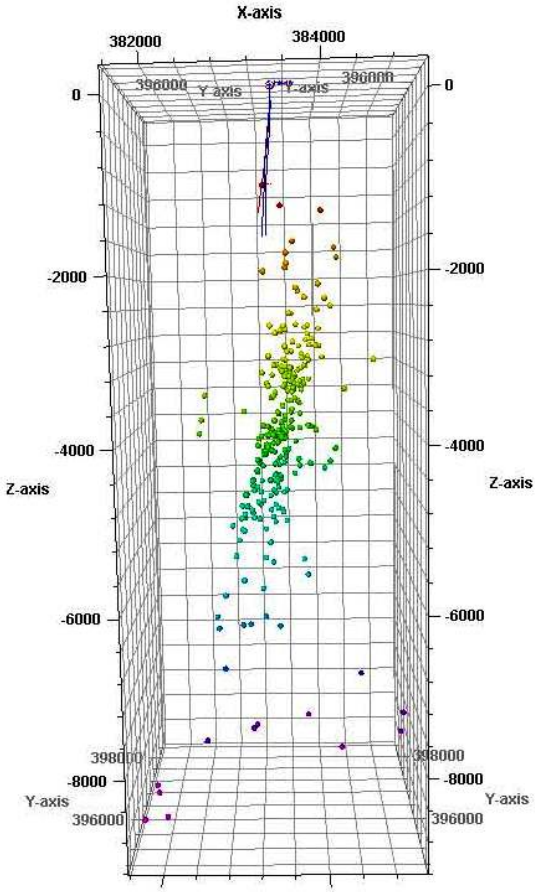

Figure 10: *Induced seismicity during circulation loss of cold water while drilling an injection well.*

The data from these latest events at Hengill were not supposed to be included and analysed within the GEISER project as they were collected late in the year 2011, the second year of GEISER. However, as this dataset is of high importance in understanding the earthquake triggering effect of large scale re-injection, an attempt is being made to use at least some of the obtained data for the GEISER work. The power company that owns the data is now organizing how these data will be treated and released to the scientific community.

Data from Reykjanes peninsula include data from two production fields, Svartsengi and Reykjanes. In Svartsengi, production has been ongoing since 1977 and re-injection started in 1984. Reykjanes entered production of 100 MW_e in 2006 but without re-injection until 2009. In addition to the national seismic network in Iceland the University of Iceland and the University of Wisconsin operated a local seismic network in Reykjanes from December 2008 until May 2009. Around 320 earthquakes have been located during that period. The seismic dataset consists of continuous waveforms from 11 seismic stations at the tip of the peninsula. The seismic activity is currently being analysed, with relocation of earthquakes using the double-difference algorithm, evaluation of focal mechanisms of the earthquakes, and investigation of the relationship with injection and production data and tectonic structures.

References

Aki, K. (1965). Maximum likelihood estimate of b in the formula logN=a-bM and its confidence limits. *Bull. Earthquake Res. Inst.*, **43**, 237–239.

Baisch S., R. Vörös, R. Weidler (2009). Investigation of fault mechanisms during geothermal reservoir stimulation experiments in Cooper Basin, Australia. *Bull. Seismol. Soc. Am.***99**(1), 148-158.

Deichmann N., J. Ernst (2009).Earthquake focal mechanisms of the induced seismicity in the 2006 and 2007 below Basel (Switzerland).*Swiss. J. Geosci.***102**, 457-466.

Diehl, T., N. Deichmann, E. Kissling, S. Husen (2009).Automatic S-wave picker for local earthquake tomography.*Bull. Seismol.Soc. Am.*, **99**(3), 1906–1920, doi:10.1785/0120080019.

Goertz-Allmann B.P., A. Goertz ,S. Wiemer(2011).Stress drop variations of induced earthquakes at the Basel geothermal site. *Geophys. Res. Let.***38**, L09308, doi:10.1029/ 2011GL047498

Makropoulos, K. C. and W. Burton (1983).Seismic risk of circum-Pacific earthquakes I. Strain energy release.*Pure Appl. Geophys.*, **121**, 247–267, doi:10.1007/BF02590137.

Oye, V. and M. Roth (2003).Automated seismic event location for hydrocarbon reservoirs.*Computers& Geosciences*, **29**, 851–863, doi:10.1016/S0098-3004(03)00088-8.

Shi, Y., and B. A. Bolt (1982).The standard error of the magnitude-frequency b-value.*Bull.Seismol. Soc. Am.*, **72**, 1677–1678.

U.S. Geological Survey and California Geological Survey (2006). Quaternary fault and fold database for the United States, accessed April 2011 from USGS web site http://earthquakes.usgs.gov/regional/qfaults/.

LIST OF ATTACHMENTS

Attachment 1:

Microseismic monitoring of the first hydraulic stimulation phase at the Paralana geothermal field, Australia.

Albaric J, Oye V, Langet N, Kuehn D, Lecomte I, Hasting M, Messeiller M, Iranpour K

Attachment 2:

Large scale aseismic motion identified through 4D P wave tomography.

Calò M, Dorbath C, Cornet F, Cuenot N (2011), Geophysical Journal International

Attachment 3:

Injection tests at the EGS reservoir of Soultz-sous-Forets. Seismic response of the GPK4 stimulations.

Calò M, Dorbath C, Frogneux M.

Attachment 4:

Stress drop variations of induced earthquakes at the Basel geothermal site

Goertz-Allmann BP, Goertz A, Wiemer S

Attachment 5:

Influence of pore-pressure on the event-size distribution of induced earthquakes

Bachmann CE, Wiemer S, Goertz-Allmann BP, Woessner J

Attachment 6:

Full Waveform Inversion of Moment Tensor Solutions of the Induced Seismicity by the Stimulation of Enhanced Geothermal Site in Basel

Peng Zhao, Volker Oye, Daniela Kühn, and Simone Cesca